

# Nucleobase–Metal Hybrid Materials: Preparation of Submicrometer-Scale, Spherical Colloidal Particles of Adenine–Gold(III) via a Supramolecular Hierarchical Self-Assembly Approach

Hui Wei, Bingling Li, Yan Du, Shaojun Dong,\* and Erkang Wang\*

State Key Laboratory of Electroanalytical Chemistry, Changchun Institute of Applied Chemistry, Chinese Academy of Sciences, Changchun, Jilin 130022, People's Republic of China, and Graduate School of the Chinese Academy of Sciences, Beijing 100039, People's Republic of China

Received January 5, 2007. Revised Manuscript Received March 7, 2007

We report a simple and effective supramolecular route for facile synthesis of submicrometer-scale, hierarchically self-assembled spherical colloidal particles of adenine–gold(III) hybrid materials at room temperature. Simple mixture of the precursor aqueous solutions of adenine and HAuCl<sub>4</sub> at room temperature could result in spontaneous formation of the hybrid colloidal particles. Optimization of the experimental conditions could yield uniform-sized, self-assembled products at 1:4 molar ration of adenine to HAuCl<sub>4</sub>. Transmission electron microscopy results reveal the formation of hierarchical self-assembled structure of the as-prepared colloidal particles. Concentration dependence, ratio dependence, time dependence, and kinetic measurements have been investigated. Moreover, spectroscopic evidence [i.e., Fourier transform infrared (FTIR) and UV–vis spectra and wide-angle X-ray scattering data] of the interaction motives causing the formation of the colloidal particles is also presented. The as-prepared nucleobase–metal hybrid materials exhibited hierarchical assembly as follows: the coordination interactions of Au(III) and N atoms in adenine could produce 2–3 nm small particles, these small particles could evolve into submicrometer spherical colloidal particles via noncovalent interaction (i.e., aromatic  $\pi$ – $\pi$  stacking of adenine), and finally the submicrometer particles could be connected together through fusion of the fringes of every independent particle. Our work here may open up new possibilities for the fabrication of noncovalent interaction colloidal particles and for the preparation of decomposable colloidal templates.

## Introduction

Organic–inorganic hybrid materials, especially organic–metal hybrid materials, play important roles in many applications, including catalysis,<sup>1</sup> biological detection,<sup>2</sup> nonlinear optics,<sup>3</sup> photoactive molecular devices,<sup>4</sup> gas storage,<sup>5</sup> and supramolecular chemistry.<sup>6–7</sup> Therefore, many functional

building blocks such as heterocyclic ligands,<sup>8</sup> dendrimers,<sup>9</sup> and fullerene<sup>10</sup> have been explored to fabricate these hybrid materials. Among them, nucleobases have been extensively studied and proven to be successful and promising building blocks to construct organic–inorganic hybrid materials because (1) the specific base-pairing and  $\pi$ – $\pi$  stacking interactions existing in the DNA double helix provide powerful recognition elements to process highly structured materials<sup>11</sup> and (2) they can coordinate to metal ions through the participation of base heterocyclic ring nitrogen atoms and keto oxygen atoms.<sup>12</sup>

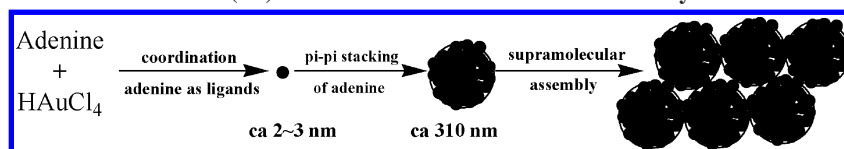
Up to now, many preparative strategies for fabricating these organic–metal hybrid materials based on supramolecular chemistry (i.e., noncovalent bonding chemistry)<sup>13</sup>

\* Address correspondence to either author: tel (+86) 431-85262003; fax (+86) 431-85689711; e-mail dongsj@ciac.jl.cn (S.D.) or ekwang@ciac.jl.cn (E.W.).

- (1) (a) Seo, J. S.; Whang, D.; Lee, H.; Jun, S. I.; Oh, J.; Jeon, Y. J.; Kim, K. *Nature* **2000**, *404*, 982–986. (b) Wight, A. P.; Davis, M. E. *Chem. Rev.* **2002**, *102*, 3598–3614.
- (2) Su, X.; Zhang, J.; Sun, L.; Koo, T.; Chan, S.; Sundararajan, N.; Yamakawa, M.; Berlin, A. A. *Nano Lett.* **2005**, *5*, 49–54.
- (3) (a) Evans, O. R.; Lin, W. *Acc. Chem. Res.* **2002**, *35*, 511–522. (b) Wang, Y.; Xie, X.; Goodson, T. *Nano Lett.* **2005**, *5*, 2379–2384.
- (4) Guldi, D. M.; Rahman, G. M. A.; Sgobba, V.; Kotov, N. A.; Bonifazi, D.; Prato, M. *J. Am. Chem. Soc.* **2006**, *128*, 2315–2323.
- (5) (a) Rosi, N. L.; Eckert, J.; Eddaoudi, M.; Vodak, D. T.; Kim, J.; O'Keefe, M.; Yaghi, O. M. *Science* **2003**, *300*, 1127–1129. (b) Rowsell, J. L.; Spencer, E. C.; Eckert, J.; Howard, J. A.; Yaghi, O. M. *Science* **2005**, *309*, 1350–1354. (c) Eddaoudi, M.; Moler, D. B.; Li, H.; Chen, B.; Reineke, T. M.; O'Keefe, M.; Yaghi, O. M. *Acc. Chem. Res.* **2001**, *34*, 319–330. (d) James, S. L. *Chem. Soc. Rev.* **2003**, *32*, 276–288.
- (6) Oh, M.; Carpenter, G. B.; Sweigart, D. A. *Acc. Chem. Res.* **2004**, *37*, 1–11.
- (7) (a) Oh, M.; Mirkin, C. A. *Nature* **2005**, *438*, 651–654. (b) Holliday, B. J.; Mirkin, C. A. *Angew. Chem., Int. Ed.* **2001**, *40*, 2022–2043. (c) Stang, P. J.; Persky, N. E.; Manna, J. J. *Am. Chem. Soc.* **1997**, *119*, 4777–4778. (d) Tabellion, F. M.; Seidel, S. R.; Arif, A. M.; Stang, P. J. *Angew. Chem., Int. Ed.* **2001**, *40*, 1529–1532.

- (8) (a) Dinolfo, P. H.; Hupp, J. T. *Chem. Mater.* **2001**, *13*, 3113–3125. (b) Clearfield, A.; Sharma, C. V. K.; Zhang, B. P. *Chem. Mater.* **2001**, *13*, 3099–3112.
- (9) (a) Garcia, M. E.; Baker, L. A.; Crooks, R. M. *Anal. Chem.* **1999**, *71*, 256–258. (b) Grohn, F.; Gu, X.; Grull, H.; Meredith, J. C.; Nisato, G.; Bauer, B. J.; Karim, A.; Amis, E. J. *Macromolecules* **2002**, *35*, 4852–4854. (c) Lemon, B. I.; Crooks, R. M. *J. Am. Chem. Soc.* **2000**, *122*, 12886–12888.
- (10) (a) Guldi, D. M.; Zilbermann, I.; Anderson, G.; Kotov, N. A.; Tagmatarchis, N.; Prato, M. *J. Am. Chem. Soc.* **2004**, *126*, 14340–14341. (b) Innocenzi, P.; Brusatin, G. *Chem. Mater.* **2001**, *13*, 3126–3139.
- (11) (a) Watson, J. D.; Crick, F. H. C. *Nature* **1953**, *171*, 737–738. (b) Seeman, N. C. *Nature* **2003**, *421*, 427–431.
- (12) Sivakova, S.; Rowan, S. J. *Chem. Soc. Rev.* **2005**, *34*, 9–21.

**Scheme 1. Schematic Representation of the Hierarchical Supramolecular Assembly from Small Nanoparticles to Large Adenine–Gold(III) Colloids and Their Final Self-Assembly Behavior**



have been developed.<sup>6,7,14</sup> These relative weak noncovalent interactions include coordination bonds,  $\pi$ – $\pi$  stacking, van der Waals forces, hydrogen bonding, electrostatic forces, hydrophobic interactions, and dipole–dipole interactions. Here we present the preparation of submicrometer-scale, nearly uniform-sized, spherical colloidal particles by employing nucleobase–metal ion interaction as a supramolecular hierarchical self-assembly motif (Scheme 1).

Self-assembly, a bottom-up technique, has been manifested as an alternative, effective, and useful fabrication method to construct ordered structures from molecular components.<sup>15</sup> Recently, much attention has been paid to synthesis of hierarchical self-assembly materials<sup>16</sup> due to their potential application in catalysis,<sup>17</sup> devices,<sup>18</sup> and sensors.<sup>19</sup> By combination of the merits of self-assembly and biological materials (such as peptides, saccharides, nucleotides, and nucleobases), novel functional materials with hierarchical order can be designed and prepared.<sup>20</sup> Although nucleobase–metal interactions have been extensively studied,<sup>21–22</sup> to the best of our knowledge, no report has so far dealt with the

preparation of submicrometer-scale particles consisting of nucleobases and metal ions. In this work we attempt to fabricate hierarchically structured materials employing nucleobase (adenine) and metal ions ( $\text{HAuCl}_4$ ) as molecular components. We found that simple mixture of the precursor aqueous solutions of adenine and  $\text{HAuCl}_4$  at room temperature could result in the spontaneous formation of a new class of nucleobase–metal ion submicrometer-scale particles. The as-prepared nucleobase–metal hybrid materials exhibited hierarchical assembly as follows (Scheme 1): the coordination interactions of  $\text{HAuCl}_4$  and adenine could produce 2–3 nm small particles, these small particles could evolve into submicrometer spherical colloidal particles via noncovalent interaction (i.e.,  $\pi$ – $\pi$  stacking), and finally the submicrometer particles could be connected together through fusion of the fringes of every independent particle. The fact that thus-formed colloidal particles can be easily broken up by a strong reducing reagent such as  $\text{NaBH}_4$  suggests a potential application as easily decomposable colloidal templates.<sup>14</sup>

## Experimental Section

**Chemicals and Materials.** Adenine, guanine, cytosine, thymine, and uracil were obtained from Chemical Reagents Research Institute (Shanghai, China). 6-(Methylamino)purine was obtained from Sigma (Milwaukee, WI). Sodium borohydride ( $\text{NaBH}_4$ ) was purchased from Aldrich (Milwaukee, WI). Chloroauric acid ( $\text{HAuCl}_4$ ) was purchased from Shanghai Chemical Reagent Co. (Shanghai, China). Other reagents and chemicals were at least analytical reagent grade. The water used throughout all experiments was purified by a Milli-Q system (Millipore, Bedford, MA).

**Instrumentation.** Transmission electron microscopy (TEM) measurements were made on a Hitachi H-8100 transmission electron microscope operated at an accelerating voltage of 200 kV. The samples for TEM characterization were prepared by placing a drop of colloidal solution on a carbon-coated copper grid and drying at room temperature. Scanning electron microscopy (SEM) measurements were made on a XL30 ESEM FEG scanning electron microscope at an accelerating voltage of 20 kV, equipped with a Phoenix energy-dispersive X-ray analyzer. The samples for SEM measurements were sputter-coated with a conductive platinum thin layer to improve the electrical conductivity. Analysis of the X-ray photoelectron spectra (XPS) was performed on an ESCLAB MKII with Mg as the exciting source. Absorption spectra were recorded on a Cary 500 scan UV–vis–NIR spectrophotometer (Varian, Harbor City, CA) at room temperature. Fourier transform infrared (FTIR) spectra were measured within the 4000–400  $\text{cm}^{-1}$  region on a Perkin-Elmer model 580B infrared spectrophotometer with the KBr pellet technique. The wide-angle X-ray scattering (WAXS) analysis was performed on a D/Max 2500 V/PC X-ray diffractometer with Cu (40 kV, 30 mA) radiation.

**Preparation of the Colloid Samples.** The  $\text{HAuCl}_4$ –adenine hybrid colloid samples were prepared according to the following procedure (sample 1): First, 1 mL of adenine aqueous solution

- (13) Lehn, J.-M. *Supramolecular Chemistry: Concepts and Perspectives*; VCH: Weinheim, Germany, 1995.
- (14) (a) Sun, X. P.; Dong, S. J.; Wang, E. K. *J. Am. Chem. Soc.* **2005**, *127*, 13102–13103. (b) Beck, J. B.; Ineman, J. M.; Rowan, S. J. *Macromolecules* **2005**, *38*, 5060–5068. (c) Zhao, H.; Heintz, R. A.; Ouyang, X.; Dunbar, K. R.; Campana, C. F.; Rogers, R. D. *Chem. Mater.* **1999**, *11*, 736–746. (d) Whitesides, G. M.; Simanek, E. E.; Mathias, J. P.; Seto, C. T.; Chin, D.; Mammen, M.; Gordon, D. A. *Acc. Chem. Res.* **1995**, *28*, 37–44.
- (15) (a) Whitesides, G. M.; Mathias, J. P.; Seto, C. T. *Science* **1991**, *254*, 1312–1319. (b) Whitesides, G. M.; Grzybowski, B. *Science* **2002**, *295*, 2418–2421. (c) Park, S.; Lim, J.-H.; Chung, S.-W.; Mirkin, C. A. *Science* **2004**, *303*, 348–351. (d) Laibinis, P. E.; Whitesides, G. M.; Allara, D. L.; Tao, Y. T.; Parikh, A. N.; Nuzzo, R. G. *J. Am. Chem. Soc.* **1991**, *113*, 7152–7167. (e) Decher, G. *Science* **1997**, *277*, 1232–1237.
- (16) (a) Zhang, W.; Liao, S. S.; Cui, F. Z. *Chem. Mater.* **2003**, *15*, 3221–3226. (b) Ferrer, M. L.; Esquembre, R.; Ortega, I.; Mateo, C. R.; del Monte, F. *Chem. Mater.* **2006**, *18*, 554–559. (c) Wright, A.; Gabaldon, J.; Burckel, D. B.; Jiang, Y.-B.; Tian, Z. R.; Liu, J.; Brinker, C. J.; Fan, H. *Chem. Mater.* **2006**, *18*, 3034–3038. (d) De Napoli, M.; Nardis, S.; Paolesse, R.; Vicente, M. G. H.; Lauceri, R.; Purrello, R. *J. Am. Chem. Soc.* **2004**, *126*, 5934–5935.
- (17) Dai, S. *Chem. Eur. J.* **2001**, *7*, 763–768.
- (18) Pileni, M. P. *J. Phys. Chem. B* **2001**, *105*, 3358–3371.
- (19) Fan, H. Y.; Yang, K.; Boye, D.; Sigmon, T.; Malloy, K.; Xu, H.; Lopez, G. P.; Brinker, C. *Science* **2004**, *304*, 567–571.
- (20) (a) Zhang, S. *Nat. Biotechnol.* **2003**, *21*, 1171–1178. (b) Lomander, A.; Hwang, W.; Zhang, S. *Nano Lett.* **2005**, *5*, 1255–1260.
- (21) (a) Gibson, D. W.; Beer, M.; Barrett, R. J. *Biochemistry* **1971**, *10*, 3669–3679. (b) Garcia-Teran, J. P.; Castillo, O.; Luque, A.; Garcia-Couceiro, U.; Roman, P.; Lezama, L. *Inorg. Chem.* **2004**, *43*, 4549–4551. (c) Demers, L. M.; Ostblom, M.; Zhang, H.; Jang, N.-H.; Liedberg, B.; Mirkin, C. A. *J. Am. Chem. Soc.* **2002**, *124*, 11248–11249. (d) Ostblom, M.; Liedberg, B.; Demers, L. M.; Mirkin, C. A. *J. Phys. Chem. B* **2005**, *109*, 15150–15160. (e) Purohit, C. S.; Verma, S. *J. Am. Chem. Soc.* **2006**, *128*, 400–401.
- (22) (a) Roitzsch, M.; Lippert, B. *Inorg. Chem.* **2004**, *43*, 5483–5485. (b) Tanaka, K.; Yamada, Y.; Shionoya, M. *J. Am. Chem. Soc.* **2002**, *124*, 8802–8803. (c) Mohan, P. J.; Datta, A.; Mallajosyula, S. S.; Pati, S. K. *J. Phys. Chem. B* **2006**, *110*, 18661–18664. (d) Dobrzynska, D.; Jerzykiewicz, L. B. *J. Am. Chem. Soc.* **2004**, *126*, 11118–11119. (e) Li, Z.; Mirkin, C. A. *J. Am. Chem. Soc.* **2005**, *127*, 11568–11569.

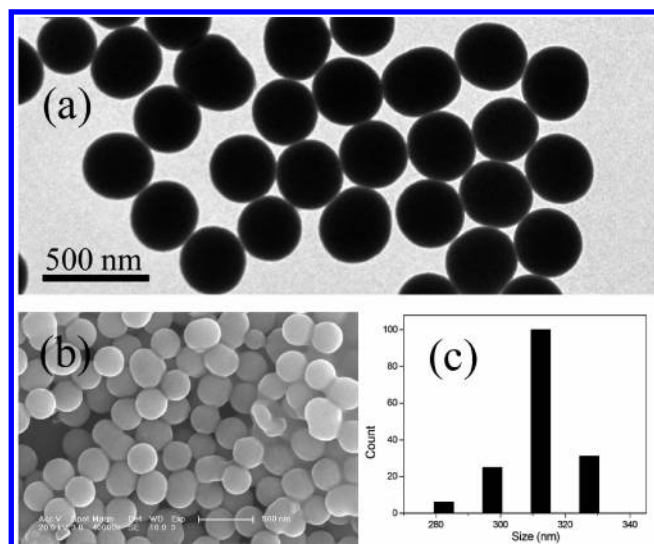


**Figure 1.** Typical TEM (a) and SEM (b) images of the as-prepared HAuCl<sub>4</sub>–adenine hybrid colloidal particles obtained at molar ratio 1:4 adenine:HAuCl<sub>4</sub> (sample 1), and corresponding size distribution histogram (c).

(10 mM) was added into 10 mL of water. HAuCl<sub>4</sub> aqueous solution (1.36 mL, 29.4 mM) with 1:4 molar ratio of adenine to HAuCl<sub>4</sub> was then introduced into the resulting solution under rigorous stirring at room temperature. A gradual color change was observed and a large amount of precipitate occurred within several minutes. The colloid solution was further stirred for another 12 h. The colloid samples thus prepared were used directly for characterization without further treatment.

To examine the influence of reactant concentration on the colloidal particles thus formed, 0.1- and 10-fold concentrations of both HAuCl<sub>4</sub> and adenine reactants were investigated, under conditions otherwise identical to those used for preparing sample 1. To examine the influence of the molar ratio of adenine to HAuCl<sub>4</sub> on the colloidal particles thus formed, the amount of HAuCl<sub>4</sub> used was investigated, under conditions otherwise identical to those used for preparing sample 1.

To examine the influence of different bases on the nucleobase–metal hybrid colloidal particles thus formed, 1 mL of bases aqueous solution (including 6-(methylamino)purine, guanine, thymine, cytosine, and uracil) (10 mM) were reacted with 1.36 mL of HAuCl<sub>4</sub> aqueous solution (29.4 mM) with molar ratio 1:4 bases:HAuCl<sub>4</sub>, under conditions otherwise identical to those used for preparing sample 1.

To decompose the as-prepared colloidal particles through redox reaction with NaBH<sub>4</sub>, 50 μL of aqueous NaBH<sub>4</sub> (5.5 mg/mL) was introduced into the as-prepared colloidal solution under rigorous stirring.

## Results and Discussion

**Hierarchical Self-Assembly of HAuCl<sub>4</sub>–Adenine Colloids.** Formation of the HAuCl<sub>4</sub>–adenine hybrid colloidal particles was confirmed by TEM and SEM data. Figure 1 depicts typical TEM (Figure 1a) and SEM images (Figure 1b) and the corresponding particle size distribution histogram (Figure 1c) of as-prepared HAuCl<sub>4</sub>–adenine hybrid colloidal particles, indicating that most of them were spherical in shape with an average diameter of 310 ± 15 nm.

It should be noted that thus-prepared colloidal particles were not separated from each other but displayed a quite interesting self-assembly phenomenon (Figure 1a). Further

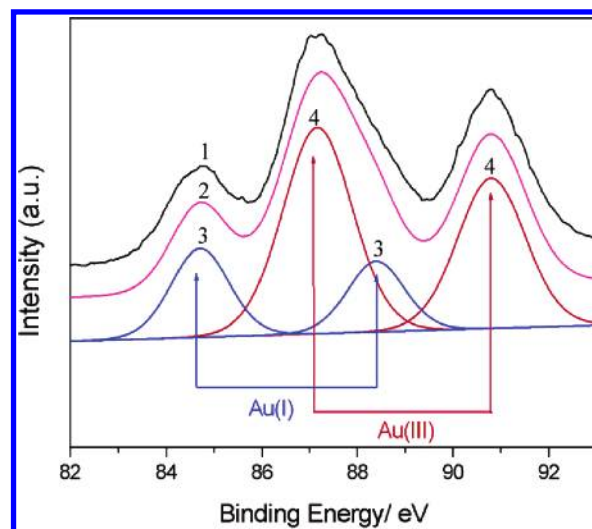


**Figure 2.** XPS spectra of Au 4f of the as-prepared HAuCl<sub>4</sub>–adenine hybrid colloidal particles (sample 1) deposited on the silica wafer: original spectrum (black line 1), whole spectrum after analysis (magenta line 2), Au(I) 4f spectrum after analysis (blue line 3), and Au(III) 4f spectrum after analysis (red line 4).

careful examination of the TEM image (Figure 1a) revealed that, in most cases, the neighboring particles were linked with each other through fusion of the fringes of every independent particle. A few particles were even fused together as shown in Figure 1a (TEM images of some twinned or triplex particles are given in Figure S1, Supporting Information). More interestingly, the hierarchical structures of the as-prepared colloidal particles could be observed at higher magnification TEM images. As depicted in Figure S2 (Supporting Information), the as-prepared 310 nm hybrid colloidal particles consisted of 2–3 nm smaller particles. The formation mechanism of such 310 nm hybrid colloidal particles and their hierarchical self-assembly behavior could be suggested as shown in Scheme 1, and the detailed evidence for this mechanism will be discussed later.

**Characterization of HAuCl<sub>4</sub>–Adenine Colloids.** For further characterization of the as-prepared 310 nm hybrid colloidal particles, energy-dispersed spectrum (EDS) and XPS spectrum analysis were carried out. The chemical composition of the resulting colloids was determined by EDS (Figure S3, Supporting Information) of the resulting colloids coated on a silicon wafer. The peaks of Au, Cl, C, and N were found (the peak of Si originated from the silicon wafer), indicating that the colloids were products of adenine and HAuCl<sub>4</sub>.

Note that the XPS spectrum of the HAuCl<sub>4</sub>–adenine hybrid colloidal particles showed three binding energy peaks in the Au 4f region at 84.7, 87.2, and 90.8 eV (Figure 2), which obviously indicated that the gold in as-prepared colloids was in the Au(I)/Au(III) mixed-valence state.<sup>23</sup> Further analysis of the XPS data gave Au 4f<sub>7/2</sub> and Au 4f<sub>5/2</sub> binding energy spectra of Au(I) and Au(III), respectively, as follows: Au(I), 84.7 (Au 4f<sub>7/2</sub>) and 88.3 (Au 4f<sub>5/2</sub>) eV; Au(III), 87.2 (Au 4f<sub>7/2</sub>) and 90.8 (Au 4f<sub>5/2</sub>) eV.<sup>24</sup> The mixed-

(23) Son, J.; Mizokawa, T.; Quilty, J. W.; Takubo, K.; Ikeda, K.; Kojima, N. *Phys. Rev. B* **2005**, *75*, 23510.

(24) Kitagawa, H.; Kojima, N.; Nakajima, T. *J. Chem. Soc., Dalton Trans.* **1991**, 3121–3125.



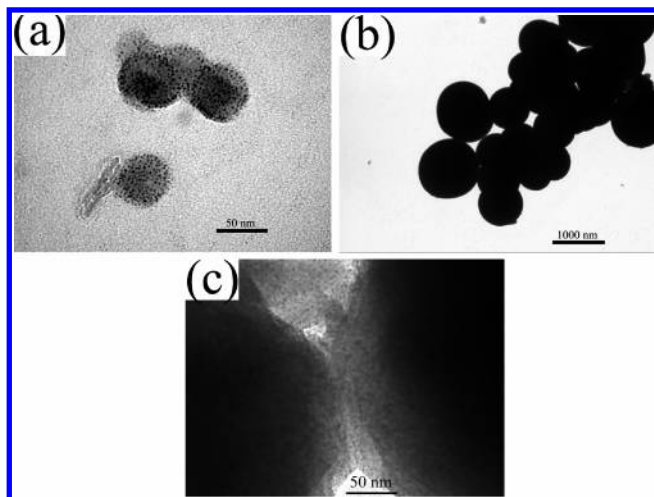


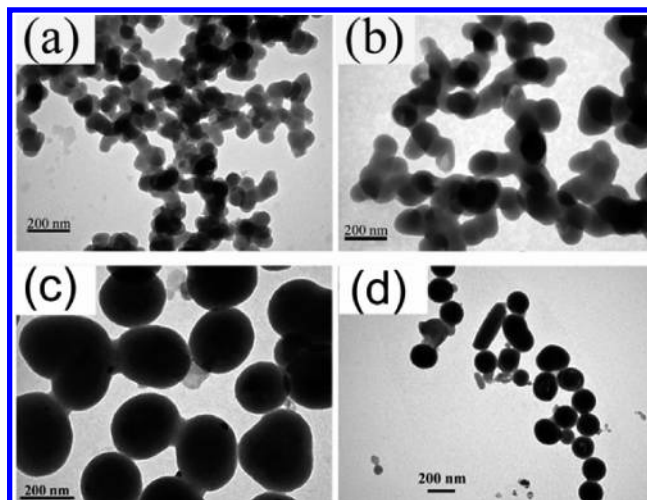
**Figure 3.** TEM images of HAuCl<sub>4</sub>-adenine hybrid colloidal particles obtained at with (a) 0.1-fold and (b) 10-fold concentration of the reactants. (c) High-magnification image of panel b.

valence state could be attributed to the following reason: the partial photoredox reaction for the HAuCl<sub>4</sub>-adenine hybrid colloidal particles by X-ray irradiation during the collection of XPS spectrum will reduce Au(III) to Au(I).<sup>14</sup> On the basis of the fact that adenine could not reduce Au(III) into Au(0)<sup>25–26</sup> and the XPS results above-mentioned, it seems reasonable to suppose that the gold element in the colloidal particles existed in its trivalent oxidation state [i.e., Au(III)].

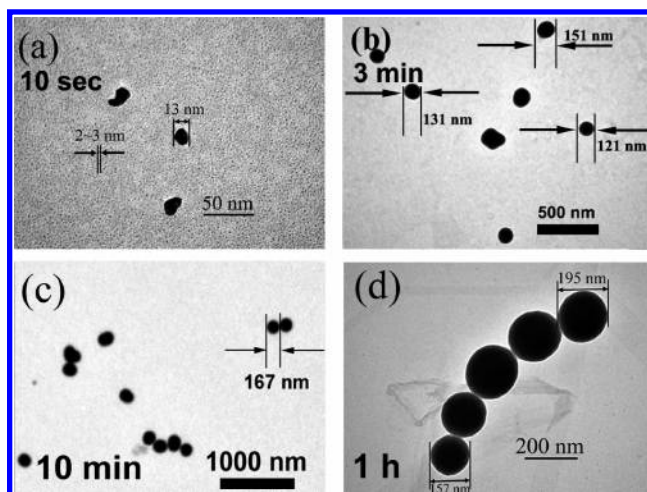
**Concentration and Ratio Dependences.** To further investigate how these 2–3 nm smaller particles evolved into the larger 310 nm hybrid colloidal particles, the influences of the concentration and molar ratio of the reactants (here HAuCl<sub>4</sub> and adenine, respectively) on the larger 310 nm colloidal particles thus formed were studied in detail.

Figure 3 shows TEM images of the colloidal particles obtained at different reactant concentrations. When the concentration was decreased to 0.1 times that of sample 1, we mainly obtained aggregated products consisting of smaller colloidal spheres with mean diameter 2–3 nm (Figure 3a). On the other hand, when the concentration increased to 10 times that of Sample 1, we observed a large quantity of polydisperse, fused spherical particles with diameter ranging from ~650 to ~1200 nm (Figure 3b). It is interesting to observe that these colloidal particles obtained at 10-fold concentration were also composed of 2–3 nm smaller particles (Figure 3c). The TEM results obtained at different reactant concentrations in Figure 3 thereby confirmed the hierarchical assembly behaviors of the hybrid colloidal particles as shown in Scheme 1.

We further examined the influence of the molar ratio of adenine to HAuCl<sub>4</sub> on the colloids thus formed by varying the amount of HAuCl<sub>4</sub> used. At 4:1 and 1:1 molar ratios, we obtained products consisting of fused, chainlike particles with mean diameter 70 and 100 nm, respectively (Figure 4a,b). However, a 1:8 molar ratio gave products mainly



**Figure 4.** TEM images of HAuCl<sub>4</sub>-adenine hybrid colloidal particles obtained at molar ratios (a) 4:1, (b) 1:1, (c) 1:8, and (d) 1:20 adenine:HAuCl<sub>4</sub>.



**Figure 5.** Time-dependent TEM images of the HAuCl<sub>4</sub>-adenine hybrid colloidal particles obtained at molar ratio 1:4 adenine:HAuCl<sub>4</sub> after reaction for (a) 10 s, (b) 3 min, (c) 10 min, and (d) 1 h.

containing a large quantity of fused spherical particles with mean diameter 220 nm and a small fraction of larger aggregated particles (Figure 4c), while a 1:20 molar ratio gave products mainly containing polydisperse spherical particles with mean diameter 170 nm (Figure 4d). A 1:4 molar ratio was an optimal option, producing uniform-sized, self-assembled spherical colloidal particles with diameter of 310 nm (Figure 1a,b).

**Time Dependence and Kinetic Measurement.** Time dependence experiments were performed to investigate the growth kinetics of hierarchical self-assembly of the as-prepared HAuCl<sub>4</sub>-adenine colloidal particles. Shown in Figure 5 (also see Figures S4–S7, Supporting Information) are the time-dependent TEM images of the colloidal particles (sample 1) obtained after different reaction times. Reaction for 10 s gave products mainly containing a large quantity of 2–3 nm small particles, as well as a few larger 13 nm particles. After 3 min reaction, we obtained products consisting of spherical particles with mean diameter 130 nm. The larger 130 nm colloidal particles could precipitate from the reaction solution. In fact, the clear yellowish reaction solution changed into macroscopic turbid yellowish solution after

(25) Steenken, S.; Jovanovic, S. V. *J. Am. Chem. Soc.* **1997**, *119*, 617–618.

(26) Lewis, F. D.; Letsinger, R. L.; Wasielewski, M. R. *Acc. Chem. Res.* **2001**, *34*, 159–170.

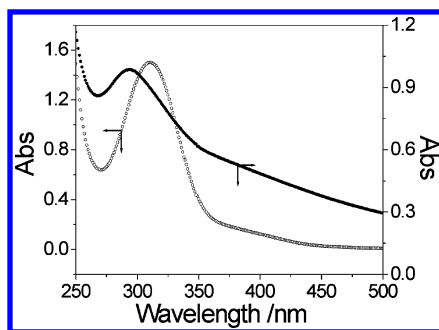


**Figure 6.** UV–visible spectra of (---) as-prepared HAuCl<sub>4</sub>–adenine hybrid colloidal particles obtained at molar ratio 1:4 adenine:HAuCl<sub>4</sub> and (—) HAuCl<sub>4</sub> alone as control.

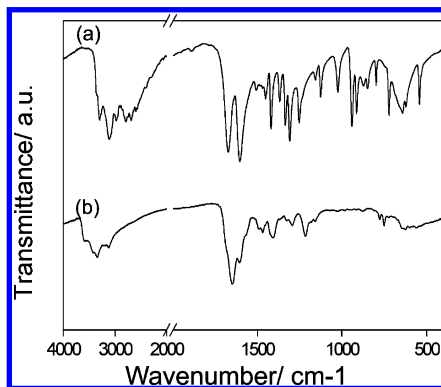


**Figure 7.** FTIR spectra of (a) adenine and (b) as-prepared HAuCl<sub>4</sub>–adenine hybrid colloidal particles obtained at molar ratio 1:4 adenine:HAuCl<sub>4</sub>.

reaction for 3 min (also see the turbidity measurements below). The particle size increased to 167 nm after reaction for 10 min and further to 210 nm after reaction for 1 h. Final products with a mean diameter of 310 nm could be obtained after reaction for 12 h (Figure 1). Clearly, the colloidal particles size increased with increasing reaction time (Figure S8a, Supporting Information).

Turbidity measurements<sup>27</sup> on a Cary 500 scan UV–vis–NIR spectrophotometer were performed to monitor the kinetics of the colloidal particle hierarchical self-assembly process. Absorption of the colloidal solutions at 600 nm was monitored as a function of reaction time. The turbidity of the reaction solution increased during the process and remained constant after about 2 h of reaction (Figure S8b, Supporting Information). In combination with the time-dependent TEM results above-mentioned, the kinetic measurements here display the hierarchical self-assembly behaviors of the colloidal particles as shown in Scheme 1 (i.e., the initial 2–3 nm smaller particles might evolve into the 310 nm hybrid colloidal particles and these 310 nm particles could further assemble through fusion of the fringes of every independent particle).

**Driving Force for Hierarchical Self-Assembly (Coordination and  $\pi$ – $\pi$  Stacking).** What is the driving force for the hierarchical self-assembly of these colloidal particles? Relatively weak noncovalent interactions such as hydrogen bonding, electrostatic forces, dipole–dipole interactions,

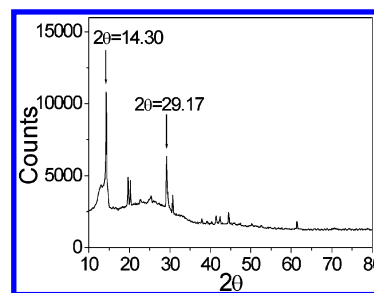


**Figure 8.** WAXS pattern of the as-prepared HAuCl<sub>4</sub>–adenine hybrid colloidal particles obtained at molar ratio 1:4 adenine:HAuCl<sub>4</sub>.

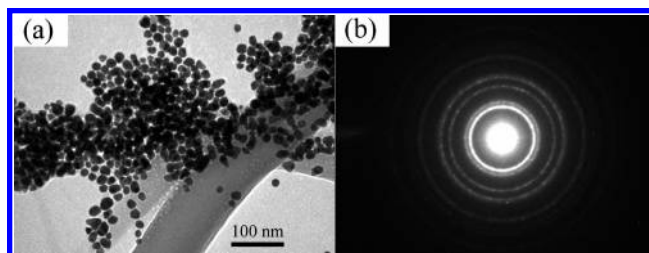


**Figure 9.** (a) TEM image of HAuCl<sub>4</sub>–guanine hybrid colloidal particles; (b) corresponding electron diffraction pattern.

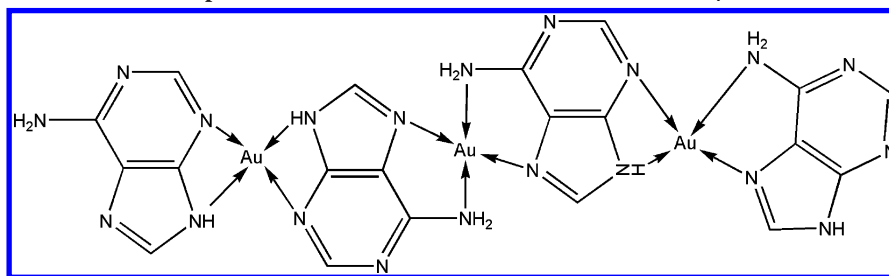
$\pi$ – $\pi$  stacking, and coordination bonds usually play important role in supramolecular chemistry.<sup>6,7,13,14,28</sup>

It is well-documented that heterocyclic ring nitrogen donor ligands can coordinate with Au(I) or Au(III) cations.<sup>29</sup> Adenine offers five main donor sites (N1, N3, N7, N9, and C6–NH<sub>2</sub>; see Figure S9, Supporting Information) for metal ion coordination.<sup>12,21,30</sup> It has been suggested that there was coordination interaction between Au(III) and adenine.<sup>21a</sup> Coordination interactions in the as-prepared HAuCl<sub>4</sub>–adenine colloidal particles could be verified by UV–vis spectra (Figure 6). A ca. 15 nm blue shift of the UV–vis spectra is indicative of the coordination reaction between HAuCl<sub>4</sub> and adenine.<sup>31</sup> The absorption peak centered at 310 nm of HAuCl<sub>4</sub> alone could be assigned to the Cl to gold charge transfer, while the absorption peak centered at 295 nm of the colloidal particles could be assigned to the N to gold charge transfer.<sup>31</sup>

The coordination interactions could be further confirmed by FTIR spectra (Figure 7 and Table S1, Supporting Information). The 1673 cm<sup>–1</sup> band of adenine was considered to arise from the NH<sub>2</sub> scissoring vibrational mode.<sup>32</sup> The corresponding NH<sub>2</sub> IR band of the colloidal particles was

- (28) Tang, Z.; Kotov, N. A.; Giersig, M. *Science* **2002**, *297*, 237–240.  
 (29) (a) Cronje, S.; Raubenheimer, H. G.; Spies, H. S. C.; Esterhuysen, C.; Schmidbaur, H.; Schier, A.; Kruger, G. *J. J. Chem. Soc., Dalton Trans.* **2003**, 2859–2866. (b) Fan, D.; Yang, C. T.; Ranford, J. D.; Vittal, J. J.; Lee, P. F. *J. Chem. Soc., Dalton Trans.* **2003**, 3376–3381.  
 (30) (a) Vrkcic, A. K.; Taverner, T.; James, P. F.; O’Hair, R. A. *J. J. Chem. Soc., Dalton Trans.* **2004**, 197–208. (b) Morikawa, M.; Yoshihara, M.; Endo, T.; Kimizuka, N. *J. Am. Chem. Soc.* **2005**, *127*, 1358–1359.  
 (31) Gangopadhyay, A. K.; Chakravorty, A. *J. J. Chem. Phys.* **1961**, *35*, 2206–2209.  
 (32) (a) Kyogoku, Y.; Lord, R. C.; Rich, A. *J. Am. Chem. Soc.* **1967**, *89*, 496–504. (b) Nowak, M. J.; Lapinski, L.; Kwiatkowski, J. S.; Leszczynski, J. *J. Phys. Chem.* **1996**, *100*, 3527–3534. (c) Silaghi, S. D. Optical Characterization of DNA Bases on Silicon Surfaces. Ph.D. Dissertation, University of Technology, Chemnitz, Germany, 2005; Chapt. 2. (d) Bukietynska, K.; Krot-Lacina, K. *Polyhedron* **2001**, *20*, 2353–2361. (e) Chatterji, D.; Nandi, U. *S. Biopolymers* **1977**, *16*, 1863–1878.

(27) (a) Bradt, J.; Mertig, M.; Teresiak, A.; Pompe, W. *Chem. Mater.* **1999**, *11*, 2694–2701. (b) Zhang, W.; Liao, S. S.; Cui, F. *Z. Chem. Mater.* **2003**, *15*, 3221–3226.

Scheme 2. Proposed Coordination Interactions between HAuCl<sub>4</sub> and Adenine

observed at 1649 cm<sup>-1</sup>. The shift of the NH<sub>2</sub> IR band could be attributed to the C6–NH<sub>2</sub> coordination with Au(III).<sup>32</sup> The shift of the C<sub>4</sub>N<sub>9</sub> IR band may suggest coordination interactions between Au(III) and N<sub>9</sub> (from 1419 cm<sup>-1</sup> in adenine to 1407 cm<sup>-1</sup> in the colloidal particles), while the disappearance of the 1125 cm<sup>-1</sup> IR band in adenine may suggest coordination interactions between Au(III) and N<sub>7</sub>.

On the basis of the above-mentioned UV–vis and IR data, we might suggest that the 2–3 nm smaller particles in the as-prepared HAuCl<sub>4</sub>–adenine colloidal particles could result from Au(III) and the N donor sites coordinate bonds through N→Au←N bridges (Schemes 1 and 2).

To further investigate how these 2–3 nm smaller particles evolved into larger 310 nm colloidal particles, WAXS measurements have been performed. Shown in Figure 8 is the WAXS pattern of the as-prepared HAuCl<sub>4</sub>–adenine hybrid colloidal particles, which gave rise to a sharp diffraction peak at 2θ = 29.17°. The corresponding interplanar spacing determined is 3.06 Å, which is comparable with the distance between two stacked adenine molecules.<sup>33</sup> The diffraction peak at 2θ = 14.30° (the corresponding interplanar spacing determined is 6.19 Å) was indicative of another orientation in addition to the aromatic rings stacking.<sup>34</sup> The π–π stacking in the colloidal particles could also be verified by addition of an aromatic solvent toluene since it could interact through π–π stacking.<sup>35</sup> Addition of toluene, which is an aromatic solvent, could indeed disrupt the 310 nm larger colloidal particles (Figure S10, Supporting Information).

Further careful examination of the TEM image (Figure S10b, Supporting Information) revealed that the disrupted colloidal aggregates consisted of 2–3 nm smaller particles. This result here provided further convincing evidence for the hierarchical self-assembly process of the as-prepared colloidal particles (Scheme 1).

Did other noncovalent interactions such as electrostatic interactions and H-bonding play roles in the formation of the hierarchical self-assembly colloidal particles? Electrostatic interactions usually play a role in colloidal systems. So we have investigated the influence of salt addition on the as-prepared colloids. As shown in Figure S11 (Supporting Information), the self-assembly structures of the as-prepared

310 nm particles still remained when K<sub>2</sub>SO<sub>4</sub> was added. This result may suggest that electrostatic contribution was insignificant in the present system.

To investigate the H-bonding interactions, FTIR measurements were performed. The FTIR spectrum (Figure 7) did not show the presence of H-bonding in the as-prepared HAuCl<sub>4</sub>–adenine hybrid colloidal particles. The perturbations of in the spectral range of 2000–400 cm<sup>-1</sup> between adenine and HAuCl<sub>4</sub>–adenine hybrid colloidal particles could be assigned to coordination interactions of Au(III) and N atoms in adenine as mentioned above. The 4000–2000 cm<sup>-1</sup> spectra were also recorded (Figure 7). In the solid spectrum of adenine alone, there was no band above 3355 cm<sup>-1</sup>, and the IR bands could be assigned to antisymmetric and symmetric stretching vibrations of the H-bonded C6–NH<sub>2</sub> and stretching vibrations of the H-bonded N9H groups.<sup>32a,b</sup> As for the as-prepared colloidal particles, the upgoing IR bands in this region may probably arise from the non-H-bonded amino group (C6–NH<sub>2</sub> and N9H) since the coordination interactions between the Au(III) and N atoms in adenine could break the H-bonding in the solid adenine alone (Scheme 2).<sup>32a,b</sup>

**Control Experiments with Other Nucleobases.** To further verify the hierarchical self-assembly mechanism above-mentioned (Schemes 1 and 2), control experiments with different bases [including 6-(methylamino)purine, guanine, thymine, cytosine, and uracil] were performed.

Mixing of HAuCl<sub>4</sub> and 6-(methylamino)purine, which is an analogue of adenine having a C6–NH<sub>2</sub> site hydrogen substitution with methyl group (Figure S9, Supporting Information), gave similar hierarchical self-assembled colloidal particles as did mixing HAuCl<sub>4</sub> and adenine (Figure S12, Supporting Information). Since 6-(methylamino)purine has as many coordination sites as adenine, the same mechanism could be suggested for the formation of the hierarchical self-assembled colloidal particles (Scheme 1).

As for guanine, mixing of HAuCl<sub>4</sub> and guanine did not form a similar kind of hierarchical self-assembled colloidal particles. Shown in Figure 9a is the typical TEM image of HAuCl<sub>4</sub>–guanine hybrid colloidal particles, which mainly consisted of 10–20 nm (diameter) particles.<sup>36</sup> The electron diffraction pattern acquired from the products in Figure 9a showed the crystalline feature of the Au nanoparticles, which implied that redox reaction between HAuCl<sub>4</sub> and guanine

(33) Silaghi, S. D. Optical Characterization of DNA Bases on Silicon Surfaces. Ph.D. Dissertation, University of Technology, Chemnitz, Germany, 2005; Chapt. 3.

(34) (a) Nolan, S. J.; Shiels, J. C.; Tuite, J. B.; Cecere, K. L.; Baranger, A. *M. J. Am. Chem. Soc.* **1999**, *121*, 8951–8952. (b) Schall, O. F.; Gokel, G. W. *J. Org. Chem.* **1996**, *61*, 1449–1458. (c) Kryachko, E. S.; Remacle, F. *J. Phys. Chem. B* **2005**, *109*, 22746–22757.

(35) (a) Sanders, G. M.; van Dijk, M.; van Veldhuizen, A.; van der Plas, H. C. *J. Org. Chem.* **1988**, *53*, 5272–5281. (b) Hunter, C. A.; Sanders, J. K. M. *J. Am. Chem. Soc.* **1990**, *112*, 5525–5534.

(36) Some large aggregates (~330 nm) and belts were also observed in the TEM images (see Figure S13). The aggregation could be assigned to the poor capping ability of guanine. The reason for formation of the belts, however, is not clear at present and needs further investigation.



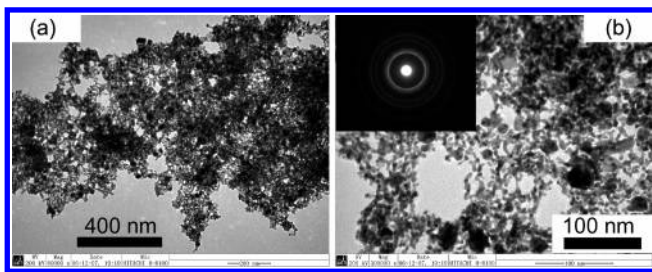


**Figure 10.** (a) TEM image of  $\text{NaBH}_4$  reduction products of as-prepared  $\text{HAuCl}_4$ -adenine hybrid colloidal particles obtained at molar ratio 1:4 adenine: $\text{HAuCl}_4$ . (b) Higher magnification image of panel a. (Inset) Electron diffraction pattern of the sample.

occurred.<sup>25,26</sup> These gold nanoparticles could not evolve into larger particles because the guanine bases were damaged during the redox reaction. Thus, the  $\pi$ - $\pi$  stacking interactions of guanine ligands could not be realized due to the possible broken of guanine aromatic structure.<sup>37</sup>

Mixing of  $\text{HAuCl}_4$  and cytosine (or thymine, or uracil), however, did not create any colloidal particle products and the reaction solutions remained clear even after 12 h of stirring. Since coordination was a prerequisite for the formation of the hierarchical self-assembled colloidal particle (Scheme 1), whether there were coordination interactions between  $\text{HAuCl}_4$  and cytosine (or thymine, or uracil) was examined by UV-vis measurements. Blue shifts of the UV-vis spectra (Figures S14–S16, Supporting Information) were indicative of coordination interactions between  $\text{HAuCl}_4$  and cytosine (or thymine, or uracil).<sup>31</sup> The question here is why these pyrimidine bases do not work. On the basis of the differences in molecular structures of these pyrimidine bases and adenine (Figure S9, Supporting Information), we suppose that, though there were coordination interactions between Au(III) and these pyrimidine bases (i.e., cytosine, thymine, and uracil), the pyrimidine ligands could not provide enough and suitable coordination sites for the  $\text{N}\rightarrow\text{Au}\leftarrow\text{N}$  bridge interactions between Au(III) and pyrimidine ligands.<sup>14</sup> Thus the mixing of  $\text{HAuCl}_4$  and the pyrimidine ligands could not evolve into 2–3 nm small particles and therein could not assemble into large colloidal aggregates.

**Mechanism of Hierarchical Self-Assembly.** On the basis of all the above-mentioned results, we suggest that coordination interactions of Au(III) and N atoms in adenine and aromatic  $\pi$ - $\pi$  stacking of adenine play dominant and cooperative roles in the supramolecular hierarchical assembly process of this  $\text{HAuCl}_4$ -adenine system (Schemes 1 and 2): (i) the coordination interactions of  $\text{HAuCl}_4$  and adenine could produce the 2–3 nm smaller particles,<sup>14,21,29,30</sup> (ii) these 2–3 nm smaller particles might evolve into the 310 nm hybrid colloidal particles through the  $\pi$ - $\pi$  stacking interactions of adenine ligands,<sup>34</sup> and (iii) assembly of the 310 nm hybrid colloidal particles could be realized through fusion of the fringes of every independent particle via supramolecular motifs.

**Reduction of the Colloidal Particles.** The as-prepared colloidal particles can be easily decomposed through redox reaction of  $\text{HAuCl}_4$  contained therein with  $\text{NaBH}_4$ . As shown

in Figure 10, reduction of the colloidal particles gave products mainly containing a large quantity of fused, chainlike gold nanoparticles with mean diameter 6–8 nm, indicating that the larger networking present at the prerelation stage was decomposed after reduction. Electron diffraction pattern acquired from the products showed the crystalline feature of the Au nanoparticles (Figure 10, inset). The disappearance of the UV-vis absorption band (295 nm) of the colloidal particles and the appearance of an SPR band (530 nm) of the Au nanoparticles further confirmed the reduction reaction (Figure S17, Supporting Information). Since template-assisted synthesis has been frequently employed to prepare shape-controlled materials from one-dimensional nanowires to three-dimensional nanostructures,<sup>38</sup> the colloidal particles fabricated in this work might be used as decomposable template for preparation of hollow-structured materials. Studies along this direction are in progress.

## Conclusion

In summary, we have demonstrated for the first time here a simple and effective hierarchical supramolecular self-assembly route for facile synthesis of submicrometer-scale, spherical colloidal particles of nucleobase-metal hybrid materials at room temperature. Optimization of the experimental conditions could yield uniform-sized, self-assembled products at 1:4 molar ration of adenine to  $\text{HAuCl}_4$ . A proper reaction mechanism was also presented. Our work here may open up new possibilities for the preparation of noncovalent interaction colloidal particles by use of nucleobases as building blocks through a mild, room-temperature supramolecular self-assembly strategy. Additionally, thus formed colloidal particles are a new class of hybrid materials with versatile properties provoked by combining the merits of two precursor compounds and might find applications in many fields.<sup>14</sup> Finally, such colloidal particles can be easily broken up by a strong reducing reagent such as  $\text{NaBH}_4$  because of the reduction of the Au cations contained therein, and therefore, they hold great promise as easily decomposable colloidal templates for wide applications.<sup>14</sup>

**Acknowledgment.** This work is supported by the NSFC, China (No. 20335040, 20675078 and 20427003) and the Chinese Academy of Sciences (No. KJCX2.YW.H09). Dr. Xingling Li is acknowledged for analysis of XPS data. Hui Wei dedicates this paper to Ms. Cunlan Guo on the occasion of her 24<sup>th</sup> birthday.

**Supporting Information Available:** Higher magnification TEM images, EDS pattern, size distribution histograms, and UV-vis spectra of the as-prepared colloidal particles, molecular structures of bases used in this study, and assignments of the FTIR spectra (PDF). This material is available free of charge via the Internet at <http://pubs.acs.org>.

CM070028A

(37) Jia, L.; Shafirovich, V.; Shapiro, R.; Geacintov, N. E.; Broyde, S. *Biochemistry* **2006**, *45*, 6644–6655.

(38) (a) Yi, G.-R.; Moon, J. H.; Yang, S.-M. *Chem. Mater.* **2001**, *13*, 2613–2618. (b) Angelatos, A. S.; Radt, B.; Caruso, F. *J. Phys. Chem. B* **2005**, *109*, 3071–3076. (c) Caruso, F.; Caruso, R. A.; Mohwald, H. *Chem. Mater.* **1999**, *11*, 3309–3314. (d) Sun, Y.; Xia, Y. *Science* **2002**, *298*, 2176–2179. (e) Yu, D.; Yam, W. V. *J. Am. Chem. Soc.* **2004**, *126*, 13200–13201.